required for adjustment to a constant back pressure slightly further downstream.

To show further flow details in a particular case, lines of constant Mach number are plotted in Fig. 3 for blades having thickness ratio 5% undergoing oscillations with frequency $\tau^{-1}=0.5$ and amplitude 2.5 deg, at a value of time when the flows in adjacent "channels" are noticeably different. The flows are seen to be nearly one-dimensional except near the entrance and exit and just behind the shock wave. The displacement of the (dashed) sonic line and the shock-wave displacement should probably both be considered $\mathcal{O}(1)$; the amplitudes, however, cannot be determined from a single plot because of the difference in the phase lags. Although $\tau^{-1}=0.5$ should be regarded as $\mathcal{O}(1)$, as already noted, it may be worth recalling that the amplitudes of the sonic-line and shock-wave motions would be predicted by the asymptotic theory of Ref. 1 to be $\mathcal{O}(1)$ if $\tau^{-1}=\mathcal{O}\{\epsilon\}$ and $\alpha=\mathcal{O}\{\epsilon^2\}$.

Concluding Remarks

The computational scheme appears successful in capturing shock waves, but is not capable of resolving vortex sheets sharply. Preliminary calculations for a staggered cascade suggest that the method will be successful for these geometries as well. The asymptotic solutions of Ref. 1 provide fairly good agreement for the shock-wave position provided that the blade thickness ratio and oscillation amplitude are both small enough. Higher-order terms are needed to improve the accuracy for a wider parameter range, and the correct inner solution at the exit is not yet understood. A broader range of numerical calculations is needed to establish whether or not the shock-wave motion has a large effect on the moment for realistic values of the parameters.

References

[1]Messiter, A. F. and Adamson, T. C., Jr., "Forced Oscillations of Transonic Channel and Inlet Flows with Shock Waves," *AIAA Journal,* Vol. 22, Nov. 1984, pp. 1590–1599.

[2]Messiter, A. F. and Adamson, T. C., Jr., "Transonic Small-Disturbance Theory for Lightly Loaded Cascades," *AIAA Journal,* Vol. 19, Aug. 1981, pp. 1047–1054.

[3]Verdon, J. M., "Linearized Unsteady Aerodynamic Theory," *AGARD Manual on Aeroelasticity in Axial Flow Turbomachines,* Vol. 1: Unsteady Turbomachinery Aerodynamics, edited by M. F. Platzer and F. O. Carta, AGARD-AG-298, 1987, Chap. 2.

[4]Acton, E. and Newton, S. G., "Numerical Methods for Unsteady Transonic Flow," *AGARD Manual on Aeroelasticity in Axial Flow Turbomachines,* Vol. 1: Unsteady Turbomachinery Aerodynamics, edited by M. F. Platzer and F. O. Carta, AGARD-AG-298, 1987, Chap. 6.

[5]Li, C.-C., "Unsteady Transonic Cascade Flows," Ph.D. Thesis, The Univ. of Michigan, Ann Arbor, MI, 1988.

[6]Adamson, T. C., Jr. and Messiter, A. F., "Asymptotic Methods for Internal Transonic Flows," NASA Transonic Symposium, 1988.

[7]Kaza, K. R. V. and Kielb, R. E., "Flutter of Turbofan Rotors with Mistuned Blades," *AIAA Journal,* Vol. 22, Nov. 1984, pp. 1618–1625.

[8]Van Leer, B., "Toward the Ultimate Conservation Difference Scheme. V. A Second-Order Sequel to Godunov's Method," *Journal of Computational Physics,* Vol. 32, 1979, pp. 101–136.

[9]Van Albada, G. D., Van Leer, B., and Roberts, W. W., Jr., "A Comparative Study of Computational Methods in Cosmic Gas Dynamics," *Astronomy and Astrophysics,* Vol. 108, 1982, pp. 76–84.

[10]Van Leer, B., "Flux-Vector Splitting for the Euler Equations," *Lecture Notes in Physics,* Vol. 170, 1982, pp. 507–512.

[11]Anderson, W. K., Thomas, J. L., and Rumsey, C. L., "Extension and Applications of Flux-Vector Splitting to Unsteady Calculations on Dynamic Meshes," AIAA Paper 87-1152-CP, 1987.

[12]Hedstrom, G. W., "Nonreflecting Boundary Conditions for Nonlinear Hyperbolic Systems," *Journal of Computational Physics,* Vol. 30, 1979, pp. 222–237.

[13]Giles, M. B., "Nonreflecting Boundary Conditions for Euler Equation Calculations," AIAA Paper 89-1942-CP, 1989.

Suppression of Vortex Asymmetry Behind Circular Cones

Wolfgang Stahl*
Deutsche Forschungsanstalt für Luft- und Raumfahrt, 3400 Goettingen, Federal Republic of Germany

Introduction and Objective

It is a well-documented fact that the flow about a slender body of revolution at zero yaw becomes asymmetric at some high angle of incidence, see e.g., Refs. [1-4]. The initially symmetrical vortex pair on the lee side rearranges into an asymmetric configuration with the asymmetry starting either at the tail of a long afterbody or near the tip of a slender pointed nose. This asymmetric flow leads to a side force acting on the body.

The similar phenomenon of an initially symmetrical vortex pair changing to an asymmetric configuration has been observed long ago on a circular, two-dimensional cylinder, set into motion impulsively in a fluid initially at rest. Behind the cylinder, a symmetrical vortex pair develops in the course of time, growing in size and moving outwards and back until an equilibrium position is reached. After some time, the vortex pair starts to move downstream again and suddenly becomes asymmetric, see e.g., L. Prandtl and O. Tietjens.[5] This type of flow, with the vortices in symmetrical arrangement, was studied theoretically by L. Foeppl[6] using an inviscid flow model. He calculated the equilibrium positions and investigated the stability of the symmetrical vortex pair with respect to small symmetric and antisymmetric displacements from the equilibrium positions (which, in the experiment, were shortly followed by asymmetry of the vortex pair). He found that the symmetrical vortex configuration is stable for symmetric and unstable for antisymmetric disturbances. Results of further theoretical studies of the development of asymmetric flows behind a two-dimensional cylinder and a cone are reported in Refs. 7 and 8, respectively.

It was thought that there was the possibility that inserting a fin between the lee-side vortices may reduce or suppress asymmetry of the vortex flow. Therefore, the flow past a slender circular cone, without and with fin, was studied qualitatively by means of flow-visualization techniques.

Experimental Program

The flow-visualization studies were partly carried out in a water tunnel at Deutsche Forschungsanstalt für Luft- und Raumfahrt (DLR), Goettingen, Federal Republic of Germany, and partly in a wind tunnel at King Fahd University of Petroleum and Minerals (KFUPM), Dhahran, Saudi Arabia. The water tunnel of DLR has a horizontal test section with a cross-sectional area of 0.25 m × 0.33 m. Maximum velocity in the empty test section is $V_\infty \cong 0.5$ m/s. The wind tunnel at KFUPM has a closed horizontal test section with a cross-sectional area of 0.8 m × 1.1 m. Maximum velocity in the empty test section is $V_\infty = 35$ m/s. The basic circular cones had

Received June 22, 1989; presented in extended form as Paper 89-3372 at the AIAA Atmospheric Flight Mechanics Conference, Boston, MA, Aug. 14–16, 1989; revision received Sept. 28, 1989.

*Scientist, Institute of Experimental Fluid Mechanics; currently Professor, Department of Mechanical Engineering, King Fahd University of Petroleum and Minerals, Dhahran 31261, Saudi Arabia. Affiliate Member AIAA.

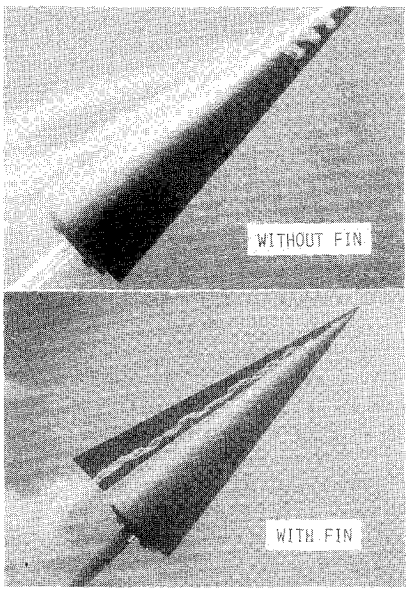

Fig. 1a Influence of lee-side fin on flow past circular cone at $\alpha = 42$ deg, $Re_D \cong 7800$ (side view).

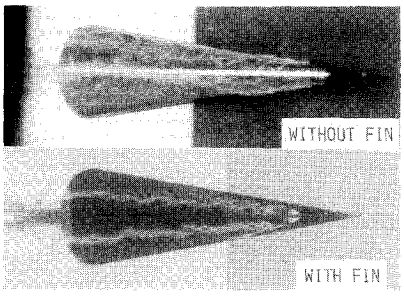

Fig. 1b Influence of lee-side fin on flow past circular cone at $\alpha = 42$ deg, $Re_D \cong 7800$ (top view).

semiapex angles $\delta_N = 8$ deg, lengths $L = 200$ mm and 500 mm, and base diameters $D = 56.2$ mm and 140.5 mm for the water tunnel and wind tunnel, respectively. To this basic configuration, a fin was added extending along the entire length of the cone. Several such fins were used protruding to heights $a/r = 1.25$, 1, 0.75, and 0.5 above the cone surface (r local radius of the cone). In the water tunnel, very small quantities of dye were applied to the model surface, with the model outside the test section. After having placed the model into the water, the flow patterns immediately became visible and were recorded on standard color film. In the wind tunnel, smoke was introduced into the flow upstream of the model. The flow patterns were made visible in laser-light planes perpendicular to the cone axis and recorded on standard color film.

Experiments were carried out on the small cone ($L = 200$ mm) in the water tunnel at angles of incidence from $\alpha = 15$ deg to $\alpha = 50$ deg; the Reynolds number formed with the base diameter D was $Re_D \cong 7800$. The tests in the wind tunnel were performed with the large model ($L = 500$ mm) at $\alpha = 45.5$ deg and $Re_D = 68{,}100$.

Results and Discussion

The influence on the lee-side vortex flow of a fin was investigated at angles of incidence $\alpha \geq 35$ deg for which the basic cone had a clearly asymmetric vortex flow.

When the fin with height $a/r = 1$ was attached to the basic cone at angles of incidence 35 deg $\leq \alpha \leq 50$ deg the hitherto asymmetric vortex configurations became, at least nominally, symmetrical. This beneficial influence of the fin on the lee-side flow becomes clearly apparent in the flow-visualization pictures. Figures 1a and 1b show typical flow patterns, at $\alpha = 42$ deg, for the cone without fin and with fin, in side view and top view. With a fin of height $a/r = 3/4$, the effect on the flow was limited to angles of incidence 35 deg $\leq \alpha \leq 40$ deg.

In order to see whether this suppression of asymmetry at relatively low Reynolds number $Re_D \cong 7800$ could also be affected at a higher Reynolds number, the flow was studied in a wind tunnel at a Reynolds number $Re_D = 68{,}100$, which is 8.7 times the previous value. Only one angle $\alpha = 45.5$ deg was considered. The vortex flow of the basic cone without fin was clearly asymmetric. Again, the addition of the fin ($a/r = 1$) resulted in a nominally symmetrical vortex configuration.

Thus, it has been experimentally established on two similar cone models with differing dimensions and tested in two different tunnels at two values of Reynolds numbers of different orders of magnitude that the addition of a fin suppresses the asymmetry of the vortex flow present without fin.

Foeppl's[6] findings for the two-dimensional cylinder, that the symmetrical vortex pair is stable for symmetric but unstable for asymmetric disturbances, may provide an explanation for the effect of the fin. If a fin is added to the cylinder between the vortices, and considering first only one of the vortices, the fin may be represented by an image vortex of the actual vortex. Together with the image vortices inside the cylinder, one has the vortex configuration as investigated with respect to stability by Foeppl. When the actual vortex is displaced in an arbitrary way, the vortex system experiences symmetric disturbances for which the vortex positions are stable. This applies to each of the two actual vortices. Foeppl already hypothesized about such an effect of a splitter plate behind a cylinder. These considerations as to the stability of the vortex configuration could possibly be carried over by means of unsteady-flow analogy to the three-dimensional vortex flow behind the corresponding inclined cylinder and qualitatively to the inclined cone, thus providing an explanation for the effect of the fin. The experiments carried out at two Reynolds numbers differing in their values by an order of magnitude showed the same stabilizing effect of the fin on the vortex flow, i.e., viscous effects seem not to influence this phenomenon suggested by inviscid flow analysis.

Conclusions

Visualization of the flow past a slender, circular cone at high incidence revealed that the addition of a fin on the lee side, in the incidence plane, essentially suppressed the asymmetry of the lee-side vortex flow. Results of an inviscid analysis of the stability of the vortex positions behind a two-dimensional circular cylinder, started impulsively, suggest a possible explanation of the experimental findings. As the asymmetric flow gives rise to a side force on the body, suppression of flow asymmetry by means of the fin lets one expect that no or only a small side force will act on the cone with fin. The investigations should be extended to more practical nose shapes and to nose-afterbody configurations to fully explore the potential offered by a fin, possibly adjustable in height, to suppress flow asymmetry and associated side force. On the other hand, one could think of using the fin in a position with insufficient height to suppress asymmetry and to exploit the associated side force for control purposes.

It was learned that work was reported concurrently[9] on a fin applied to a nose, suppressing asymmetry.

Acknowledgments

The support of this work by DLR and KFUPM, especially by the respective staff in the workshops, laboratories, and offices is gratefully acknowledged.

References

[1]Allen, H. J., and Perkins, E. W., "Characteristics of Flow Over Inclined Bodies of Revolution," NACA, RM A50L07, March 1951.

[2]Fiechter, M., "Wirbelsysteme schlanker Rotationskörper und die aerodynamischen Kräfte," *DGLR*, Jahrbuch, 1969, pp. 77–85.

[3]Hunt, B. L., "Asymmetric Vortex Forces and Wakes on Slender Bodies," AIAA Paper 82-1336, Aug. 1982.

[4]Kompenhans, J., and Hartmann, K., "Strömungssichtbarmachung an einem hochangestellten Ogivkreiszylinderrumpf mit Hilfe der Laser-Lichtschnittmethode," DFVLR-FB 86-45, 1986.

[5]Prandtl, L., and Tietjens, O., *Applied Hydro- and Aeromechanics*, McGraw-Hill, New York and London, 1934.

[6]Foeppl, L., "Wirbelbewegung hinter einem Kreiszylinder," Sitz.ber., Königl. Bay. Akademie d. Wissenschaften, Math.-Phys. Klasse, Jg. 1913, München, Jan. 1913.

[7]Sun, Y. C., Shen, S. F., and Zhu, Z., "A Numerical Simulation of the Flow Development Behind a Circular Cylinder Started from Rest and a Criterion for Investigating Unsteady Separating Flows," *Acta Mechanica*, Vol. 71, Jan. 1988, pp. 1–20.

[8]Dyer, D. E., Fiddes, S. P., and Smith, J. H. B., "Asymmetric Vortex Formation From Cones at Incidence—A Simple Inviscid Model," *Aeronautical Quarterly*, Vol. 33, Nov. 1982, pp. 293–312.

[9]Ng, T., "On Leading Edge Vortex and Its Control," AIAA Paper 89-3346, Aug. 1989.

Theoretical Foundation of the Equations for the Generation of Surface Coordinates

Z. U. A. Warsi*

Mississippi State University, Mississippi State, Mississippi

Nomenclature†

$b_{\alpha\beta}$ = $\mathbf{n}\cdot\mathbf{r}_{,\alpha\beta}$; coefficients of the second fundamental form

D = second-order differential operator; Eq. (2)

G_ν = $g_{\alpha\alpha}g_{\beta\beta}-(g_{\alpha\beta})^2$, (α,β,ν) cyclic, e.g., $G_3=g_{11}g_{22}-(g_{12})^2$

$g_{\alpha\beta}$ = $\mathbf{r}_{,\alpha}\cdot\mathbf{r}_{,\beta}$; covariant metric components

$g^{\alpha\beta}$ = contravariant metric components

$g^{\alpha\sigma}g_{\beta\sigma}$ = δ^α_β; thus, $g^{11}=g_{22}/G_3$, $g^{12}=-g_{12}/G_3$, $g^{22}=g_{11}/G_3$

k_I, k_{II} = principal curvatures at a point in the surface

$\mathbf{n}$ = $(\mathbf{r}_{,\alpha}\times\mathbf{r}_{,\beta})/(\sqrt{G_\nu})$; unit normal vector on the surface (x^ν = const, e.g., $\nu=3$: $\alpha=1$, $\beta=2$)

$\mathbf{r}$ = (x_i); $i=1, 2, 3$, the Cartesian coordinates

R = defined in Eq. (4)

x^α = two dimensional curvilinear coordinates; (α, β, ν) cyclic

x^ν = const, defines the surface; $\nu=1,2,3$

$\Upsilon^\delta_{\alpha\beta}$ = $\frac{1}{2}g^{\sigma\delta}(g_{\alpha\sigma,\beta}+g_{\beta\sigma,\alpha}-g_{\alpha\beta,\sigma})$; surface Christoffel symbols of the second kind

Δ_2 = $\dfrac{1}{\sqrt{G_3}}\dfrac{\partial}{\partial x^\alpha}\left((\sqrt{G_3})g^{\alpha\beta}\dfrac{\partial}{\partial x^\beta}\right)$, Beltramian/Laplacian Operator

Received Oct. 25, 1988; revision received April 25, 1989.

*Professor, Department of Aerospace Engineering. Member AIAA.

†Greek indicates (except ν) assume two values. A comma before a suffix, say α, indicates a partial derivative with respect to the curvilinear coordinate x^α. Thus, $\mathbf{r}_{,\alpha}=\delta\mathbf{r}/\delta x^\alpha$, $\mathbf{r}_{,\alpha\beta}=\delta^2\mathbf{r}/\delta x^\alpha\delta x^\beta$. On the other hand, a variable subscript denotes a partial derivative, e.g., $\mathbf{r}_\xi=\delta\mathbf{r}/\delta\xi$, $\mathbf{r}_\nu=\delta\mathbf{r}/\delta\nu$, etc. Summation convention is implied when the same index appears both as a lower and an upper index.

Introduction

DESPITE the availability of a large body of literature on elliptic grid generation, there has not been much discussion on the foundational aspects of the model equations which are used to generate the grid lines. It always appears that the equations, called the grid generators, have been chosen on an ad hoc basis except when the grids are to be generated in the two-dimensional physical x-y space. In the later case early authors (e.g., Winslow,[1] Chu,[2] and Thompson et al.[3]) chose the Laplace equations as the grid generators based on their simplicity and above all because of the existence of a maximum principle for such equations. Brackbill,[4] in search of a criteria for grid smoothness on the basis of a variational principle, again established that the Laplace equations form the most optimum grid generators for the two-dimensional physical x-y space. It is when one tries to develop a set of elliptic grid generators for a curved surface in the three-dimensional physical x, y, z space that the whole question on the foundational aspect again comes forward. Warsi[5–8] has proposed a set of elliptic partial differential equations that are based on some simple differential-geometric results. In essence, the starting point of the works in Refs. 5–8 is the fact that the coordinates to be generated in a surface must satisfy the equations of Gauss, viz., Eq. (A1). (Refer to the Appendix for some essential formulas.) Besides the equations of Gauss, the surface grid equations must also satisfy the equations of Weingarten, viz., Eq. (A2). It is the purpose of this Note to show that the model proposed in Refs. 5–8 also satisfies the equations of Weingarten. With the satisfaction of the preceding equations, the proposed model equations for the surface have a fundamental basis and thus form an optimum set of grid generators.

Model for Coordinate Generation

In this section we first use only Eq. (A1) (method I) and obtain the coordinate generation equations. Next, we use only Eq. (A2) (method II) and again obtain the same equations.

Method I

Inner multiplication of Eq. (A1) by $g^{\alpha\beta}$ and the use of the results

$$\Delta_2 x^\delta=-g^{\alpha\beta}\Upsilon^\delta_{\alpha\beta},\qquad k_I+k_{II}=g^{\alpha\beta}b_{\alpha\beta}$$

yields the equation

$$g^{\alpha\beta}\mathbf{r}_{,\alpha\beta}+(\Delta_2 x^\delta)\mathbf{r}_{,\delta}=\mathbf{n}(k_I+k_{II}) \tag{1}$$

Writing $x^1=\xi$, $x^2=\eta$, introducing the operator D

$$D=g_{22}\partial_{\xi\xi}-2g_{12}\partial_{\xi\eta}+g_{11}\partial_{\eta\eta} \tag{2}$$

and $P=\Delta_2\xi$, $Q=\Delta_2\eta$, Eq. (1) becomes

$$D\mathbf{r}+G_3(P\mathbf{r}_\xi+Q\mathbf{r}_\eta)=\mathbf{n}R \tag{3}$$

where

$$R=G_3(k_I+k_{II})=g_{22}b_{11}-2g_{12}b_{12}+g_{11}b_{22} \tag{4}$$

Equation (3) provides three scalar equations for the determination of x, y, z. To obtain a deterministic set of equations from Eq. (3), we have to prescribe the Beltramians $\Delta_2\xi$, $\Delta_2\eta$.